NANO LETTERS

Letter

pubs.acs.org/NanoLett

Hydrodynamic Slip on DNA Observed by Optical Tweezers-Controlled Translocation Experiments with Solid-State and Lipid-Coated Nanopores

Lukas Galla,[†] Andreas J. Meyer,[‡] Andre Spiering,[†] Andy Sischka,*[,†] Michael Mayer,[§] Adam R. Hall,[∥] Peter Reimann,[‡] and Dario Anselmetti[†]

[†]Experimental Biophysics and Applied Nanoscience, Faculty of Physics, Bielefeld University, 33615 Bielefeld, Germany

[‡]Theoretical Physics, Bielefeld University, 33615 Bielefeld, Germany

[§]Department of Chemical Engineering and Department of Biomedical Engineering, University of Michigan, Ann Arbor, Michigan 48109, United States

[∥]Department of Biomedical Engineering and Comprehensive Cancer Center, Wake Forest University School of Medicine, Winston Salem, North Carolina 27157, United States

ABSTRACT: We use optical tweezers to investigate the threading force on a single dsDNA molecule inside silicon-nitride nanopores between 6 and 70 nm in diameter, as well as lipid-coated solid-state nanopores. We observe a strong increase of the threading force for decreasing nanopore size that can be attributed to a significant reduction in the electroosmotic flow (EOF), which opposes the electrophoresis. Additionally, we show that the EOF can also be reduced by coating the nanopore wall with an electrically neutral lipid bilayer, resulting in an 85% increase in threading force. All experimental findings can be described by a quantitative theoretical model that incorporates a hydrodynamic slip effect on the DNA surface with a slip length of 0.5 nm.

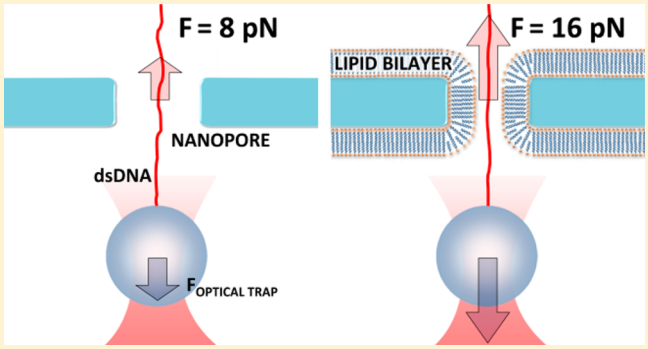

KEYWORDS: *Lipid-coated solid-state nanopores, DNA translocation, optical tweezers, electroosmotic flow, slip length*

During electrically driven translocation of DNA or other charged molecules through nanopores (NPs)[1−3] the molecule itself experiences not only an electrophoretic force but also an electroosmotic force. The latter originates from a movement of counterions at the surface of both the charged molecule and the NP side wall[4−6] and is thus strongly affected by the surface charges.[7] In addition to charge considerations, the magnitude of the electroosmotic flow (EOF) acting on a DNA molecule inside a NP decreases as pore diameter is reduced, increasing the net threading force.[8−10] Therefore, NP surface charge and diameter are important parameters for controlling the magnitude and direction of the effective threading force acting on a molecule inside a NP.

In this paper, we employ optical tweezers to investigate the threading force of an externally applied electric field acting on a double-stranded DNA (dsDNA) molecule in a silicon-nitride solid-state NP. In particular, we explore the dependence of the threading force on the pore diameter, as well as the modifications of the threading force after coating the membrane and nanopore walls with a lipid bilayer, which significantly reduces the surface charge density. As NP diameter decreases, we observe a pronounced increase in net force acting on the molecule. In addition, we find that this force almost doubles as a result of lipid-coating. To interpret these findings theoretically, we model the system in terms of the well-established Poisson, Nernst−Planck, and Stokes equations. To explain the experimental forces quantitatively, non-negligible hydrodynamic slip effects on the DNA surface are determined to be an indispensable prerequisite. This key result of our work is further corroborated by the well-known hydrophobicity of the DNA grooves and by analogous findings in recent atomistic molecular-dynamics simulations.[5,11]

Experimental Setup and Methods. Single NPs with a diameter between 6 and 70 nm were drilled by helium-ion microscopy (HIM) into a freestanding 10 (Norcada Inc., Canada), 20, or 50 nm (Structure Probe Inc., PA) thin silicon-nitride membrane as described before.[12,13] The chip containing the NP was then cleaned for 30 min in 80 °C hot piranha solution consisting of freshly mixed aqueous H_2O_2 solution and concentrated H_2SO_4 with a ratio of 1:3 (v/v), which makes the membrane hydrophilic. Afterward, the chip was carefully rinsed with deionized water and mounted into our sample chamber.

Received: May 22, 2014
Revised: June 11, 2014
Published: June 17, 2014

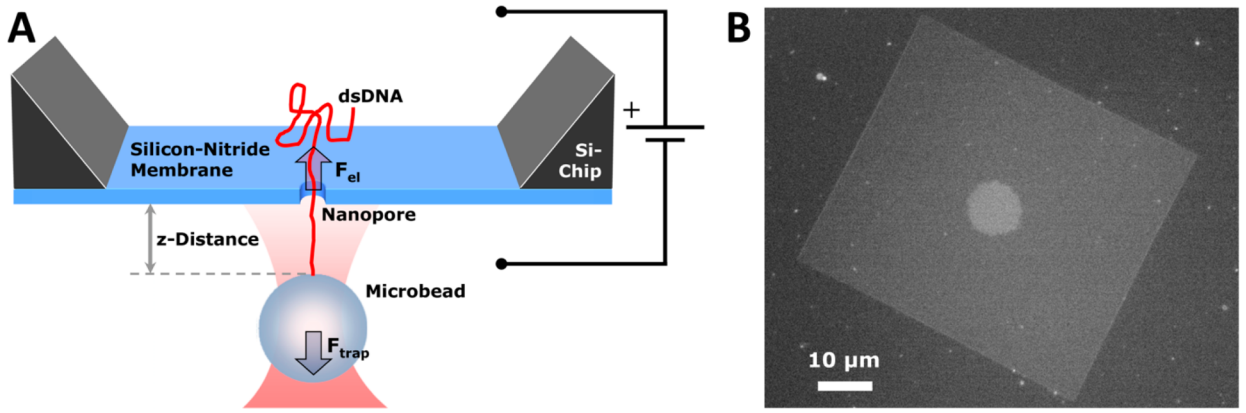

Figure 1. (A) Experimental setup. A Si-chip carries a silicon-nitride membrane with a nanopore through which a single dsDNA molecule is threaded. The DNA immobilized on the microbead experiences a net electrical force, which is balanced by the optical trapping force holding the microbead. (B) Fluorescence image of the lipid bilayer, which completely coats one side of the rectangular silicon nitride membrane. The round flake in the center of the image indicates that the lipid bilayer has moved through the nanopore and is now also coating the wall of the pore and the opposite side of the membrane.

We filled the sample chamber with a solution of 2 M KCl and 10 mM Tris/HCl at pH 8.0, measured the ionic current through the pore, and calculated the NP's electrical resistance to determine the NP diameter according to the work of Yusko et al.[14] Subsequently, the sample chamber was rinsed with our NP-buffer solution (20 mM KCl and 2 mM Tris/HCl at pH 8.0). Afterward, we introduced to the bottom compartment of the sample chamber NP-buffer solution containing 3.05 μm polystyrene microbeads (Spherotech, IL) conjugated with λ-DNA molecules (48.8 kbp, Roche Diagnostics, Germany).[15] Then, optical tweezers were used to navigate the bead-DNA construct into close proximity with the NP (Figure 1A) and a membrane voltage of +50 mV was applied across the pore. The force threading the DNA into the NP and acting on the trapped bead was measured via our video-based force detection setup.[16]

Coating of the NP walls with a lipid bilayer from small unilamellar vesicles (SUVs) and confirmation of bilayer stability was performed as detailed in ref 14. In brief, the SUVs are prepared by using a rotary evaporator to form a lipid film in a round-bottom glass flask. After resuspending this film in buffer (150 mM KCl and 10 mM HEPES at pH 7.5) to a final lipid concentration of 2 mM, SUVs were formed via tip sonication (10−20 min at 30% power). The lipid mixture was composed of 99.2 mol % POPC (1-palmitoyl-2-oleoyl-*sn*-glycero-3-phosphocholine) and 0.8 mol % DOPE labeled with Rhodamine B (1,2-dioleoyl-*sn*-glycero-3-phosphoethanolamine-N-(lissamine rhodamine B sulfonyl)), both obtained from Avanti Polar Lipids.

To coat the silicon-nitride membrane with a lipid bilayer, the sample chamber was first rinsed with buffer (150 mM KCl and 10 mM HEPES at pH 7.5), followed by exchanging the buffer in the bottom channel with the immersion of SUVs. We waited 15 min to let the vesicles interact with the silicon-nitride membrane. Because of the hydrophilic membrane, the SUVs burst on the surface, merge to a bilayer, and cover the membrane including the NP walls with a lipid bilayer. After removing excess SUVs by rinsing with deionized water, the entire sample chamber was filled with a solution of 2 M KCl and 10 mM Tris/HCl at pH 8.0 and the successful bilayer coating of the membrane and the NP wall was confirmed by characterizing fluorescence recovery after photobleaching (FRAP). The lipid bilayer not only covered the lower side of the membrane and the NP wall, but also the upper side of the membrane, forming a large flake with a typical size between 5 and 20 μm that was clearly visible by fluorescence microscopy (Figure 1B). When applying a considerable voltage of >1 V, we were able to shrink or grow this flake depending on the polarity, confirming the fluidity of the bilayer coating. As evidence of the reduced NP diameter due to the lipid-coated pore walls, we measured a reduced NP conductivity compared to the uncoated pore.[14] Subsequently, the entire sample chamber was rinsed again with NP buffer solution before we added a suspension of bead-DNA constructs into the bottom compartment to repeat the DNA threading and force measurements with the lipid-coated NP.

As far as the relatively small voltages employed in our actual force measurements are concerned, we did not observe any notable change in size and shape of the flake (Figure 1B) when comparing the fluorescence images before and after a force measurement. This fact suggest that the lipid coating may possibly exhibit some transient motion relatively to its silicon-nitride support after switching on the (relatively small) external voltage, and symmetrically after switching off the voltage, while under the steady voltage conditions of our experiment any such systematic motion of the lipid coating will have died out. Regarding the remaining possibility of random (Brownian) lipid motion, the pertinent diffusion coefficient reported in ref 14 for coatings containing POPC is 1.34 ± 0.22 nm$^2/\mu$s. Again, such a diffusive lipid motion is negligibly small in comparison with the typical ambient fluid velocities due to EOF. In summary, in the context of our present force measurements, the lipid coatings can be considered as practically immobile.

Theoretical Methods. The dynamics of DNA in a solid-state NP are governed by a complex interplay of several electrohydrodynamic effects.[4,9,17−19] The externally applied voltage generates both an electrophoretic force on the charged molecule and an electroosmotic fluid flow of the ambient electrolyte solution.[5,6] Additionally, significant forces result from self-energy,[20−22] concentration polarization,[23] counterion pressure,[24,25] and various nonlinear or charge-induced electrokinetic effects.[26] All of these particular effects will be fully contained in our theoretical model approach below.

Because the membrane is insulating, we note that the various electrohydrodynamic factors mentioned above are most pronounced within the nanopore and in its immediate vicinity.[9,18,27] In contrast, for distances d from the pore much

dx.doi.org/10.1021/nl501909t | *Nano Lett.* 2014, 14, 4176−4182

larger than the pore diameter both the electric and the EOF field decay as $1/d^2$.[18] As a consequence of this slow algebraic decay, these fields still contribute significantly to the total (integrated) force on an elongated, charged object like DNA. Accordingly, theoretical results for infinitely long pores[5,6,9,11,17] are of limited reliability for the quantitative interpretation of experimentally measured forces. Rather, the theoretical model should also take into account fairly extended fluid "reservoirs" beyond the actual pore region, as will be done in the following.

Our approach is based on the well-established framework of the coupled Poisson, Nernst–Planck, and Stokes equations,[25,28–30] which we briefly summarize in the following (for a more detailed account see e.g. ref 25). Inside the electrolyte solution, the electric potential $\psi(x)$ satisfies Poisson's equation $\varepsilon_s \Delta\psi(x) = -\rho(x)$, where $\rho(x) = F_c[c_+(x) - c_-(x)]$ is the total charge density due to the local concentrations $c_\pm(x)$ of the dissolved $K^+$and Cl^- ions, $\varepsilon_s = 80\varepsilon_0$ is the permittivity of the solution, and F_c is Faraday's constant. The DNA molecule is modeled as an elongated rod-shaped particle with a homogeneous surface charge density σ_p equivalent to the 2 electron charges per base pair of a real dsDNA (for more details, see below). Accordingly, Poisson's equation takes the form $\Delta\psi(x) = 0$ inside the particle, completed by the standard boundary condition $n\cdot[\varepsilon_s \mathbf{E}_s - \varepsilon_p \mathbf{E}_p] = \sigma_p$ at the interface between solution and particle,[25,31] where n indicates the surface normal, $\mathbf{E}_{s/p}$ is the electric field $\mathbf{E}(x) = -\nabla\psi(x)$ at the respective sides of the interface, and ε_p is the particle's permittivity, henceforth approximated as $\varepsilon_p = 2\varepsilon_0$. Analogously $\Delta\psi(x) = 0$ inside the membrane and $n\cdot[\varepsilon_s E_s - \varepsilon_m E_m] = \sigma_m$ at the membrane-solution interface, where σ_m is the surface charge density of the membrane, and $\varepsilon_m = 2\varepsilon_0$ its approximate permittivity. Finally, the experimentally applied voltage of 50 mV is taken into account via the boundary conditions $\psi = 50$ mV at the top electrode and $\psi = 0$ V at the bottom electrode (corresponding to top and bottom boundaries in Figure 2). The detailed properties of the side walls of the reservoir are of minor relevance and are accounted for by the boundary condition $n\cdot E(x) = 0$.[31]

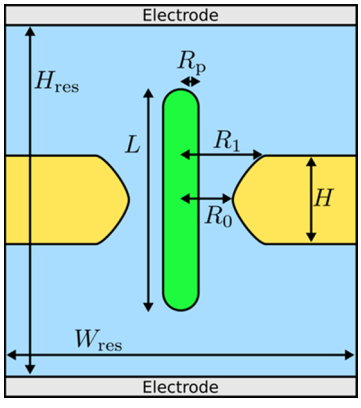

Figure 2. Schematic illustration of our theoretical model. A membrane of thickness H separates two reservoirs with electrolyte solution and is perforated by an hourglass-shaped pore with minimal and maximal radii R_0 and R_1. A rod-shaped particle of length L and radius R_p represents the part of the dsDNA molecule inside the NP and its vicinity. The entire setup is rotationally symmetric about the particle axis with overall height H_{res} and diameter W_{res}. The top and bottom boundaries of the system consist of electrodes and are subject to an externally applied voltage.

The Nernst–Planck equation $J_\pm(x) = c_\pm(x)u(x) + \mu_\pm c_\pm(x)E(x) - D_\pm \nabla c_\pm(x)$ expresses the flux densities $J_\pm(x)$ of the two ionic species in terms of their concentrations $c_\pm(x)$, their diffusion coefficients $D_\pm$ and mobilities $\mu_\pm = q_\pm D_\pm / k_B T$, and the fluid-velocity field $u(x)$.[28] Here, $q_+ = -q_- = e$ are the ion charges for K^+ and Cl^-, e is the electron charge, k_B is Boltzmann's constant, and $T = 293$ K is the temperature. In the stationary state, $\nabla J_\pm(x) = 0$ with boundary conditions $c_\pm(x) = c_0$ at the electrodes and $n\cdot J_\pm(x) = 0$ at all other boundaries,[25,28] where c_0 is the experimentally given bulk concentration of the ions far from the membrane.

Finally, the fluid velocity $u(x)$ and the pressure $p(x)$ satisfy Stokes' equation $\eta\Delta u(x) = \nabla p(x) - \rho(x)\mathbf{E}(x)$ with $\nabla u(x) = 0$ (incompressible fluid) and $\eta = 8 \times 10^{-4}$ Pa s (water viscosity at room temperature).[28] At the electrode boundaries, we assume a vanishing normal stress, that is, $\mathbf{A}n = 0$, where $\mathbf{A}$ is the hydrodynamic stress tensor with components $A_{ij} = \eta(\partial u_i/\partial x_j + \partial u_j/\partial x_i) - p\delta_{ij}$.[28] At the membrane surfaces and the side walls of the reservoirs, we adopt standard no-slip boundary conditions $u(x) = 0$ (see also end of section Experimental Setup and Methods).

Concerning the particle surface, we do not impose no-slip boundary conditions a priori. Rather, we allow for the possibility of non-negligible hydrodynamic slip effects by employing more general, so-called Navier boundary conditions $u_\parallel = l_{slip}\partial_\perp u(x)$ and $u(x)\cdot n = 0$, where $u_\parallel$ denotes the slip velocity parallel to the surface, l_{slip} is the so-called slip length, and $\partial_\perp u(x)$ the derivative of the velocity field along the direction normal to the particle surface.[32]

Once these coupled partial differential equations are solved, the main observable in the experiment, namely the net electrohydrodynamic force $\mathbf{F}$ acting on the particle, can be readily obtained as the integral $\mathbf{F} = \int_S [\mathbf{A}(x) + \mathbf{M}(x)]n\, dS$ over the particle surface S, where A is the hydrodynamic stress tensor (see above) and M is the Maxwell stress tensor with components $M_{ij} = \varepsilon_s(E_i E_j - \delta_{ij}|\mathbf{E}|^2/2)$.[31]

We have solved the above-mentioned Poisson, Nernst–Planck, and Stokes equations numerically for an axisymmetric geometry as sketched in Figure 2. The height and diameter of the total system (cylindrical container) were $H_{res} = 1$ μm and $W_{res} = 2$ μm, respectively, and we verified that further increasing these values did not notably change the results.

In our model, the membrane thickness is $H = 20$ nm in the case of the uncoated, and $H = 30$ nm in the case of the lipid-coated NP (see next section), and we verified that varying H between 10 and 60 nm changed the results by not more than 3%. The typically hourglass shape of pores was approximated as hyperboloids with minimal and maximal radii R_0 and R_1 (see Figure 2 and ref 33; in addition, the intersection of hyperboloid and flat membrane was slightly "rounded"). The minimal radius R_0 in our model was adopted to the experimentally estimated pore radius, while the maximal pore radius R_1 was kept fixed relative to R_0 as $R_1 = R_0 + H/10$ (other realistic choices of R_1 changed the results by less than 5%).

The DNA was modeled as a rod-shaped particle of radius $R_p = 1.1$ nm and length $L = 2l_{Kuhn} + H$ with a Kuhn length of $l_{Kuhn} \approx 100$ nm (= 2 × persistence length of dsDNA), thus approximating the respective literature values for dsDNA.[19,34] Likewise, we assumed a homogeneous surface charge density $\sigma_p = -2e/(0.34\text{ nm } 2\pi\ 1.1\text{ nm})$, approximating the 2 electron charges per base pair (with base pair distance of 0.34 nm and dsDNA circumference of 2π 1.1 nm). The rod-shaped DNA-molecule was positioned symmetrically along the pore axis, thus

dx.doi.org/10.1021/nl501909t | Nano Lett. 2014, 14, 4176–4182

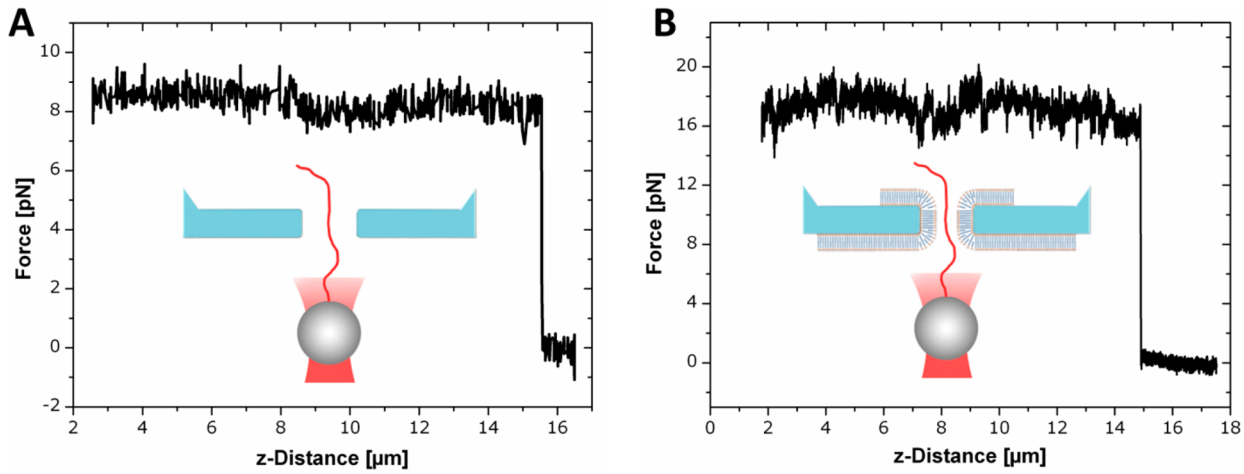

Figure 3. (A) Measured threading force on dsDNA induced by the electric field for an uncoated silicon-nitride membrane with a NP of 41 nm diameter and an applied voltage of 50 mV. As the z-distance between bead and membrane is continuously increased, the force remains constant until it instantaneously drops to zero when the dsDNA is completely pulled out of the pore. (B) Small unilamellar vesicles form a lipid bilayer-coating on both sides of the silicon-nitride membrane and nanopore walls and thus reduce the pore diameter by about 10 nm. Upon DNA threading, the measured force is significantly higher than for an uncoated pore under equal conditions.

sticking out on both sides of the pore by l_{Kuhn}. Moreover, we verified that the total force on the rod remained almost unchanged when the rod length was increased further.

Our approximation of the DNA as a rigid rod along the pore axis can be further justified as follows. Because of the opposing forces exerted on the DNA by the microbead and the NP (see Figure 1A), an approximate straight shape of this DNA-segment seems immediately plausible (indeed the distance between pore and bead at which the DNA is completely pulled out of the pore in Figure 3A, namely 15.5 μm, is very close to the nominal DNA contour length of 16.4 μm). The remaining DNA-segment on the opposite side of the NP is subjected to the above-mentioned, relatively slowly decaying electrical and EOF fields. Hence, also this segment will maintain an approximate straight shape for at least one Kuhn length. As mentioned above, increasing the length of this straight segment even further hardly changed the total force on the rod. In other words, the detailed shape of the DNA (coiled or straight) beyond one Kuhn length seems of minor importance. The same conclusion follows from the experimental observation in Figure 3A that the measured force on the DNA hardly changed as a function of the distance z between bead and NP: if DNA-coiling would play any notable role (on either side of the pore), one would expect measurable variations of the force when changing the length of the coiled DNA segment. Taking for granted that the DNA can be satisfactorily approximated by a rigid rod parallel to the pore axis, there still remains the possibility that the rod axis may deviate from the pore axis. Again, we verified that such deviations only have a minor effect on the total force on the rod, both for the uncoated and the coated NPs (see also section Theoretical Results and Discussion).

The choice of the remaining model parameters c_0, $D_{\pm}$, σ_m and l_{slip} will be discussed later.

Experimental Results and Discussion. Figure 3A shows the threading force on a typical dsDNA in an uncoated, 41 nm diameter NP with an applied voltage of 50 mV. When increasing the vertical distance z between the upper edge of the bead and the NP (see Figure 1A), a constant force of about 8 pN is observed until the DNA-strand is completely pulled out of the pore and the force drops to zero. This occurs near the contour length of the λ-DNA (16.4 μm). By this finding, we can exclude varying hydrodynamic forces acting on the bead or the portion of the dsDNA stretching between the bead and the NP. This experiment was repeated several times for NPs with different diameters and applied voltages. All measured forces depended approximately linearly on voltage over a range from 20 to 100 mV and the respective DNA threading force did not fluctuate by more than 10% when the bead was moved toward the pore to a distance z of at least 2 μm, indicating that the thermal influence of the trapping laser on the threading force is negligible.

The electrostatic component of the total force acting on dsDNA inside the NP can be estimated to be 1 pN/mV,[35] however all DNA threading experiments yield a significantly lower effective threading force.[10,12,15,16,35] This is due to the hydrodynamic coupling of the EOF pointing in the opposite direction of the electrostatic force and therefore leading to a strongly reduced measured threading force.[8] The EOF itself has its origin in the movement of the thin layer of counterions surrounding the charged DNA backbone. The EOF not only induces a drag force on the dsDNA but also on an uncharged[8] NP wall, whereupon the interplay between both drag forces lead to a gradually increasing EOF (i.e., decreasing total force[9,10]) with increasing NP diameter. Our results (Figure 4) verify this finding. Furthermore, for pores with similar diameters we found the threading force to be essentially independent of the membrane thickness in a range between 10 and 50 nm.

For NPs with a diameter smaller than 10 nm, the measured force rises to between 0.35 and 0.5 pN/mV. These values are considerably larger than measurements using pores of comparable size formed either in a 60 nm thick $SiO_2/SiN_X/SiO_2$ membrane[9] or in a 20 nm thin SiN_X membrane that was additionally thermally oxidized before use.[10] We suppose that the SiO_2 layer may lead to a stronger EOF in comparison to a bare SiN_X NP wall. Additionally, the pore manufacturing process may play a significant role in establishing the surface charge of the NP wall. We expect that the ablation ratio between nitrogen and silicon atoms[36] could differ based on the

dx.doi.org/10.1021/nl501909t | Nano Lett. 2014, 14, 4176−4182

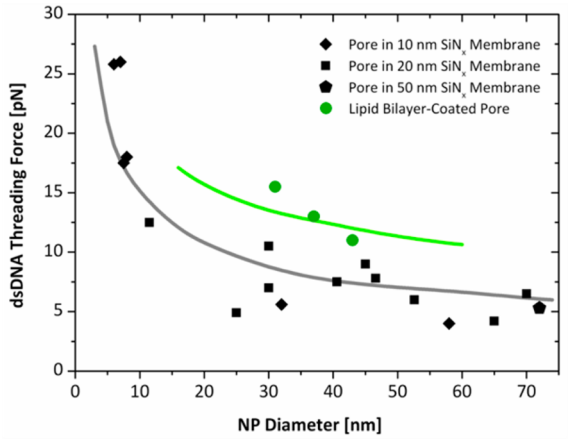

Figure 4. Relationship between dsDNA threading force (50 mV applied voltage) and the respective uncoated NP diameter (black symbols). Various membrane thicknesses are used, as indicated. All experiments are performed in a buffer solution containing 20 mM KCl and 2 mM Tris/HCl at pH 8.0. Our theoretical model for an uncoated pore (gray line) fits best to the experimental data when the silicon-nitride membrane has a negative surface charge density of $\sigma_m = -60$ mC/m^2 and when we introduce a hydrodynamic slip effect on the DNA surface with a slip length of $l_{slip} = 0.5$ nm (see text for more details). Coating the silicon nitride pore with a lipid bilayer significantly increases the threading force (green symbols). The best fit (green line) of our theoretical model for a lipid-coated pore includes a DNA slip length of 0.5 nm and a neutral surface charge density $\sigma_m = 0$ mC/m^2 of the lipid bilayer.

use of a helium ion beam (as in our experiment) as opposed to an electron beam, which would affect the surface charge and hence the EOF.

The theoretical expressions from references[9,37] for the net forces acting on a dsDNA molecule inside a NP also yield a dependency on the pore size. However, predicted forces are 50% higher than the experimental results due to the assumption of an electrically neutral NP surface.[9,37] This discrepancy can be solved by including a negative surface charge on the NP wall,[7,9,37] reducing the threading force by providing an additional component to the EOF.

To examine how an altered pore surface charge influences the EOF and the threading force, we coated the silicon nitride membrane and the NP wall with an electrically neutral lipid bilayer[14] and performed dsDNA threading experiments as described above. In particular, we confirmed the successful coating of the NP wall and the formation of a bilayer on both sides of the membrane via FRAP by adding 0.8 mol % DOPE labeled with Rhodamine B as fluorescence marker to the lipid before SUV formation and by monitoring the change of the ionic current through the pore before and after bilayer coating. Then, dsDNA was threaded through the coated NP under the same salt and pH conditions as used for uncoated pores. For each coated pore, several DNA-molecules were threaded in and out, while the threading forces were measured for each molecule and for various applied voltages. All threading forces depended approximately linearly on the applied voltage in a range between 20 and 80 mV and did not fluctuate by more than 15% during time or when approaching or retracting the bead from the pore.

Figure 3B shows the dsDNA threading force for an applied voltage of 50 mV in a lipid-coated pore (uncoated diameter 41 nm). The force rises significantly to 15.5 pN, which is about twice as large as for an uncoated pore of the same diameter. This increase can be only partially attributed to the reduction of the pore diameter due to the coating, which is 9.6 nm for POPC[14] and results in a pore diameter of about 31 nm. Because such a change in NP size would only account for a small increase in measured force, we therefore propose that the large force is primarily attributed to a significant reduction in the EOF through the pore. Because of the electrically neutral NP wall coating, the EOF caused by the negatively charged silicon nitride NP wall is suppressed, which in turn raises the total threading force. Interestingly, this force magnitude is not 50% larger as would be predicted for an uncharged NP wall,[9,37] but 85%. We obtain this value from the following three coated pores, each of which exhibit an increase of the threading force after coating: from 0.12 to 0.22 pN/mV (coated NP diameter of 43 nm), from 0.16 to 0.26 pN/mV (coated NP diameter of 37 nm), and from 0.15 to 0.31 pN/mV (coated NP diameter of 31 nm).

During DNA-unthreading no significant drop of the ionic current signal was observable, both for lipid-coated and uncoated NPs with comparable diameter.

Theoretical Results and Discussion. To quantitatively explain these experimental findings by means of the electro-hydrodynamic theory described above, we first examine the lipid-coated pores. Following recent work,[14,38,39] there is an approximately 1−2 nm thick fluid layer between the solid-state membrane material and the lipid bilayer. As a consequence, the surface charge of the solid-state membrane is strongly shielded by the counterions inside this fluid layer (Debye screening). Hence, the resulting effective surface charge of the coated membrane is expected to be negligibly small (in particular, the lipid-coating itself does not exhibit any notable surface charge of its own).

Thus, setting $\sigma_m = 0$, we find that our theory consistently underestimates the forces observed experimentally when adopting no-slip boundary conditions for the rod-shaped particle modeling the dsDNA (i.e., for $l_{slip} = 0$ nm). In particular, varying membrane thicknesses, pore shapes, as well as particle and membrane permittivities within experimentally realistic limits do not help to explain the experimental findings. Also, assuming an effective reduction of the DNA charge (see, e.g., refs 5, 6, 17, and 40−43) only increases the discrepancy between theory and experiment.

As a further possibility, we explored how the threading force changes when the particle axis is permitted to deviate from the pore axis. Because this case requires a full three-dimensional numerical solution of our theoretical model, we had to restrict ourselves to much smaller reservoirs and rods than in the axialsymmetric case. Within this restriction, we observed only minor force variations upon variation of the distance between particle and pore axis. We do not expect significantly stronger variations for longer rods and larger reservoirs.[19]

For this reason, we introduce a finite slip length l_{slip} at the DNA−particle surface. As Figure 4 (green line) demonstrates, a slip length of $l_{slip} = 0.5$ nm leads to a good quantitative agreement of the experimental results. The occurrence of such a hydrodynamic slip effect at the DNA surface is physically justified as follows: First, the common homogeneous rod model[4,9,17,37,19] clearly oversimplifies some important structural properties of the actual dsDNA. Whereas the negatively charged phosphate groups of the DNA backbone are hydrophilic, the nucleobases inside the grooves of the double helix are hydrophobic. Such hydrophobic surfaces are known to

dx.doi.org/10.1021/nl501909t | Nano Lett. 2014, 14, 4176−4182

give rise to significant hydrodynamic slip effects,[32] which may persist even in the presence of a nanoscopic substructure of alternating hydrophilic and hydrophobic domains. Second, recent atomistic molecular dynamic simulations, incorporating the detailed DNA structure, directly confirm nonzero fluid velocities along the DNA backbone.[5,11] In fact, our best fit l_{slip} = 0.5 nm agrees very well with the slip length deducible, for example, from Figure 2 in ref 11.

We recall that the lipid coating itself can be considered as practically immobile (see end of section Experimental Setup and Methods). Hence, no appreciable slip effect is expected to occur on those coated surfaces.

Next, we examine the experimental findings for the uncoated solid-state membranes. While l_{slip} = 0.5 nm is a property of the DNA model and as such must remain unchanged, an essential difference compared to the coated membranes is the negative surface charge density σ_m of the silicon nitride membrane and NP walls, typically estimated to be 15−60 mC/m^2 for our present experimental conditions.[6,44−48] Thus, considering σ_m as a fit parameter, Figure 4 (gray line) depicts our best fit to the experimental data, obtained for σ_m = −60 mC/m^2. We find that reasonable modifications to pore shape, membrane thickness, and DNA and membrane permittivities only change these results by a few percent.

In all the theoretical results described here, we employ the established approximations $D_{\pm}$ = 2 × 10^{-9} m^2/s for the K^+ and Cl^- diffusion coefficients $D_{\pm}$.[49] Upon varying $D_{\pm}$ between 1.5 to 2.5 × 10^{-9}m^2/s, the resulting curves remain indistinguishable from those in Figure 4. Likewise, the ion bulk concentrations c_0 are set to the experimental conditions c_0 = 20 mM and variations in expected force remain below 5% when using other c_0 values between 10 and 50 mM, in agreement with ref 9.

In conclusion, we utilized optical tweezers to investigate threading forces acting on a single dsDNA molecule inside both a bare silicon nitride NP and a lipid-coated solid-state NP. We measured a strong increase in the threading force upon decreasing the diameter of the bare NPs, which we attribute to a significant reduction of the EOF. Likewise, after coating the NP walls with an electrically neutral lipid bilayer the EOF is significantly reduced, resulting in an 85% increased threading force. We used electrohydrodynamic theory that adopts Poisson, Nernst−Planck, and Stokes equations to describe our experimental results and discussed the effects of reasonable modifications to the model, as well as different surface charge values and slip effects. We found that the incorporation of a hydrodynamic slip length of l_{slip} = 0.5 nm on the DNA surface explains the investigated threading force for both untreated and lipid bilayer coated NP. This suggests that the nanostructure of the DNA (hydrophilic phosphate groups and hydrophobic grooves) has to be considered for understanding the dynamics of polyelectrolytes in the highly confined environment of a NP.

AUTHOR INFORMATION

Corresponding Author

*E-mail: andy.sischka@physik.uni-bielefeld.de. Address: Universitätsstraße 25, 33615 Bielefeld, Germany.

Author Contributions

L.G., A.J.M., A.S., and A.S. contributed equally.

Notes

The authors declare no competing financial interest.

ACKNOWLEDGMENTS

This work was supported by Deutsche Forschungsgemeinschaft (DFG) under the Collaborative Research Center SFB 613 and RE1344/8-1, and by the Paderborn Center for Parallel Computing.

REFERENCES

(1) Howorka, S.; Cheley, S.; Bayley, H. *Nat. Biotechnol.* **2001**, *19*, 636.
(2) Nakane, J. J.; Akeson, M.; Marziali, A. *J. Phys.: Condens. Matter* **2003**, *15*, R1365.
(3) Miles, B. N.; Ivanov, A. P.; Wilson, K. A.; Dogan, F.; Japrung, D.; Edel, J. B. *Chem. Soc. Rev.* **2013**, *42*, 15.
(4) Ghosal, S. *Phys. Rev. E* **2006**, *74*, 041901.
(5) Luan, B.; Aksimentiev, A. *Phys. Rev. E* **2008**, *78*, 021912.
(6) He, Y.; Tsutsui, M.; Fan, C.; Taniguchi, M.; Kawai, T. *ACS Nano* **2011**, *5*, 5509−5516.
(7) Luan, B.; Aksimentiev, A. *J. Phys.: Condens. Matter* **2010**, *22*, 454123.
(8) Keyser, U. F.; van Dorp, S.; Lemay, S. G. *Chem. Soc. Rev.* **2010**, *39*, 939−947.
(9) van Dorp, S.; Keyser, U. F.; Dekker, N. H.; Dekker, C.; Lemay, S. G. *Nat. Phys.* **2009**, *5*, 347−351.
(10) van den Hout, M.; Vilfan, I. D.; Hage, S.; Dekker, N. H. *Nano Lett.* **2010**, *10*, 701−707.
(11) Kesselheim, S.; Mueller, W.; Holm, C. *Phys. Rev. Lett.* **2014**, *112*, 018101.
(12) Spiering, A.; Getfert, S.; Sischka, A.; Reimann, P.; Anselmetti, D. *Nano Lett.* **2011**, *11*, 2978−2982.
(13) Yang, J.; Ferranti, D. C.; Stern, L. A.; Sanford, C. A.; Huang, J.; Ren, Z.; Qin, L.-C.; Hall, A. R. *Nanotechnology* **2011**, *22*, 285310.
(14) Yusko, E. C.; Johnson, J. M.; Majd, S.; Prangkio, P.; Rollins, R. C.; Li, J.; Yang, J.; Mayer, M. *Nat. Nanotechnol.* **2011**, *6*, 253−260.
(15) Sischka, A.; Spiering, A.; Khaksar, M.; Laxa, M.; König, J.; Dietz, K.-J.; Anselmetti, D. *J. Phys.: Condens. Matter* **2010**, *22*, 454121.
(16) Knust, S.; Spiering, A.; Vieker, H.; Beyer, A.; Gölzhäuser, A.; Tönsing, K.; Sischka, A.; Anselmetti, D. *Rev. Sci. Instrum.* **2012**, *83*, 103704.
(17) Ghosal, S. *Phys. Rev. Lett.* **2007**, *98*, 238104.
(18) Wanunu, M.; Morrison, W.; Rabin, Y.; Grosberg, A. Y.; Meller, A. *Nat. Nanotechnol.* **2010**, *5*, 160.
(19) Lu, B.; Hoogerheide, D. P.; Zhao, Q.; Dapeng, Y. *Phys. Rev. E* **2012**, *86*, 011921.
(20) Parsegian, A. *Nature* **1969**, *221*, 844.
(21) Jordan, P. C.; Bacquet, R. J.; McCammon, J. A.; Tran, P. *Biophys. J.* **1989**, *55*, 1041.
(22) Bonthuis, D. J.; Zhang, J.; Hornblower, B.; Mathe, J.; Shklovskii, B. I.; Meller, A. *Phys. Rev. Lett.* **2006**, *97*, 128104.
(23) Das, S.; Dubsky, P.; van den Berg, A.; Eijkel, J. C. T. *Phys. Rev. Lett.* **2012**, *108*, 138101.
(24) Sader, J. E.; Chan, D. Y. C. *Langmuir* **2000**, *16*, 324.
(25) Getfert, S.; Töws, T.; Reimann, P. *Phys. Rev. E* **2013**, *88*, 052710.
(26) Bazant, M. Z.; Squires, R. M. *Curr. Opin. Colloid Interface Sci.* **2010**, *104*, 159.
(27) Zhang, J.; Shklovskii, B. I. *Phys. Rev. E* **2007**, *75*, 021906.
(28) Masliyah, J. H.; Bhattacharjee, S. *Electrokinetic and Colloid Transport Phenomena*; John Wiley & Sons: New York, 2006.
(29) Eisenberg, R. S. *J. Membr. Biol.* **1996**, *150*, 1.
(30) Corry, B.; Kuyucak, S.; Chung, S. *Biophys. J.* **2000**, *78*, 2364.
(31) Jackson, J. D. *Classical Electrodynamics*; Wiley-VCH: Weinheim, Germany, 1998.
(32) Bocquet, L.; Barrat, J.-L. *Soft Matter* **2007**, *3*, 685.
(33) Kowalczyk, S. W.; Grosberg, A. Y.; Rabin, Y.; Dekker, C. *Nanotechnology* **2011**, *22*, 315101.
(34) Hagerman, P. J. *Annu. Rev. Biophys. Biophys. Chem.* **1988**, *17*, 265.

(35) Keyser, U. F.; Koeleman, B. N.; van Dorp, S.; Krapf, D.; Smeets, R. M. M.; Lemay, S. G.; Dekker, N. H.; Dekker, C. *Nat. Phys.* **2006**, *2*, 473−477.
(36) Wu, M.; Smeets, R. M. M.; Zandbergen, M.; Ziese, U.; Krapf, D.; Batson, P. E.; Dekker, N. H.; Dekker, C.; Zandbergen, H. W. *Nano Lett.* **2009**, *9*, 479−484.
(37) Ghosal, S. *Phys. Rev. E* **2007**, *76*, 061916.
(38) Bayerl, T. M.; Bloom, M. *Biophys. J.* **1990**, *58*, 357.
(39) Miller, C. E.; Majewski, J.; Gog, T.; Kuhl, T. L. *Phys. Rev. Lett.* **2005**, *94*, 238104.
(40) Parsegian, V. A. *Annu. Rev. Biophys. Bioeng.* **1973**, *2*, 221.
(41) Rabin, Y.; Tanaka, M. *Phys. Rev. Lett.* **2005**, *94*, 148103.
(42) Hall, A. R.; van Dorp, S.; Lemay, S. G.; Dekker, C. *Nano Lett.* **2009**, *9*, 4441.
(43) Kowalczyk, S. W.; Wells, D. B.; Aksimentiev, A.; Dekker, C. *Nano Lett.* **2012**, *12*, 1038.
(44) Behrens, S. H.; Grier, D. G. *J. Chem. Phys.* **2001**, *115*, 6716.
(45) Stein, D.; Kruithof, M.; Dekker, C. *Phys. Rev. Lett.* **2004**, *93*, 035901.
(46) Kirby, B. J.; Hasselbrink, E. F. *Electrophoresis* **2004**, *25*, 187.
(47) Hoogerheide, D. P.; Garaj, S.; Golovchenko, J. A. *Phys. Rev. Lett.* **2009**, *102*, 256804.
(48) Andersen, M. B.; Frey, J.; Pennathur, S.; Bruus, H. J. *Colloid Interface Sci.* **2011**, *353*, 301.
(49) Bruus, H. *Theoretical Microfluidics*; Oxford University Press: Oxford, U.K., 2008.